REPORT

ORGANIC CHEMISTRY

Synthesis of a carbon nanobelt

Guillaume Povie,[1,2,3] Yasutomo Segawa,[1,2]* Taishi Nishihara,[1,2] Yuhei Miyauchi,[1,2,4] Kenichiro Itami[1,2,3,5]*

The synthesis of a carbon nanobelt, comprising a closed loop of fully fused edge-sharing benzene rings, has been an elusive goal in organic chemistry for more than 60 years. Here we report the synthesis of one such compound through iterative Wittig reactions followed by a nickel-mediated aryl-aryl coupling reaction. The cylindrical shape of its belt structure was confirmed by x-ray crystallography, and its fundamental optoelectronic properties were elucidated by ultraviolet-visible absorption, fluorescence, and Raman spectroscopic studies, as well as theoretical calculations. This molecule could potentially serve as a seed for the preparation of structurally well-defined carbon nanotubes.

Belt-shaped compounds consisting solely of fused benzene rings, or carbon nanobelts, were proposed as potentially game-changing molecules in chemistry (Fig. 1A) (*1*, *2*) even before the discovery of carbon nanotubes (CNTs) in 1991 (*3*). For example, cyclacene, the shortest belt segment of zigzag CNTs, appeared in the literature in 1954 as a hypothetical molecule for theoretical study (*4*). Although the groups of Stoddart (*5*), Schlüter (*6*), and Cory (*7*), as well as our group (*8*) and others, have targeted cyclacene and its derivatives, synthetic attempts toward such zigzag nanobelts have failed (*1*, *2*). In parallel to these campaigns, Vögtle proposed an armchair nanobelt (also known as a Vögtle belt), representing a segment of armchair CNTs, and initiated studies into the synthesis of this structure in the 1980s (*9*). Inspired by this goal set by Vögtle, many groups, including those of Herges (*10*), Iyoda (*11*), Bodwell (*12*), and Scott (*13*), have described extensive efforts to access various armchair nanobelts, but none have succeeded. Unlike the case of these fully fused, edge-sharing carbon nanobelts, the chemistry of carbon nanorings (arenes linked by single bonds) has burgeoned in recent years (Fig. 1B) (*14*). Cycloparaphenylenes (CPPs) were first synthesized in 2008, and since then, a number of CPP-related carbon nanorings, including potential precursors to carbon nanobelts, have been synthesized by the groups of Jasti, Yamago, Isobe, and Müllen, as well as our group and many others (*14*). However, attempts to convert those precursors into carbon nanobelts have been thwarted, mainly by strain-relieving rearrangement reactions (*15*). Iyoda's group came closest to isolating a carbon nanobelt in their observation of the mass peak of [10]cyclophenacene upon laser irradiation of a *Z*-ethenylene–bridged macrocycle (Fig. 1C) (*11*). Using a distinct strategy, Scott *et al.* succeeded in the synthesis of a CNT end-cap (*16*), and the groups of Nakamura (*17*) and Gan (*18*) extracted the substructures of nanobelts by multiaddition reactions to C_{60} and C_{70}, respectively (Fig. 1D).

Building on the knowledge, strategies, and methods accumulated through these efforts, here we report the bottom-up synthesis and isolation of carbon nanobelt **1** (Fig. 2). This compound represents a belt segment of (6,6)CNT and is an isomer of [12]cyclophenacene. The strain energy of **1** (119.5 kcal mol^{-1}) estimated by density function theory (DFT) calculation (see the supplementary materials for details) is almost the same as that of [12]cyclophenacene (115.1 kcal mol^{-1}) (*19*). The synthetic route to **1** (Fig. 2) consisted of sequential Wittig reactions for the construction of the key macrocycle **2** and a subsequent nickel(0)-mediated aryl-aryl coupling reaction. This route was inspired by Iyoda *et al.*'s extensive studies of the all-*Z*-benzannulenes (*11*) and the synthesis of strained π-systems reported by Stępień's group (*20*).

The synthesis started with benzylic bromide **3** and aldehyde **4**, both of which were easily

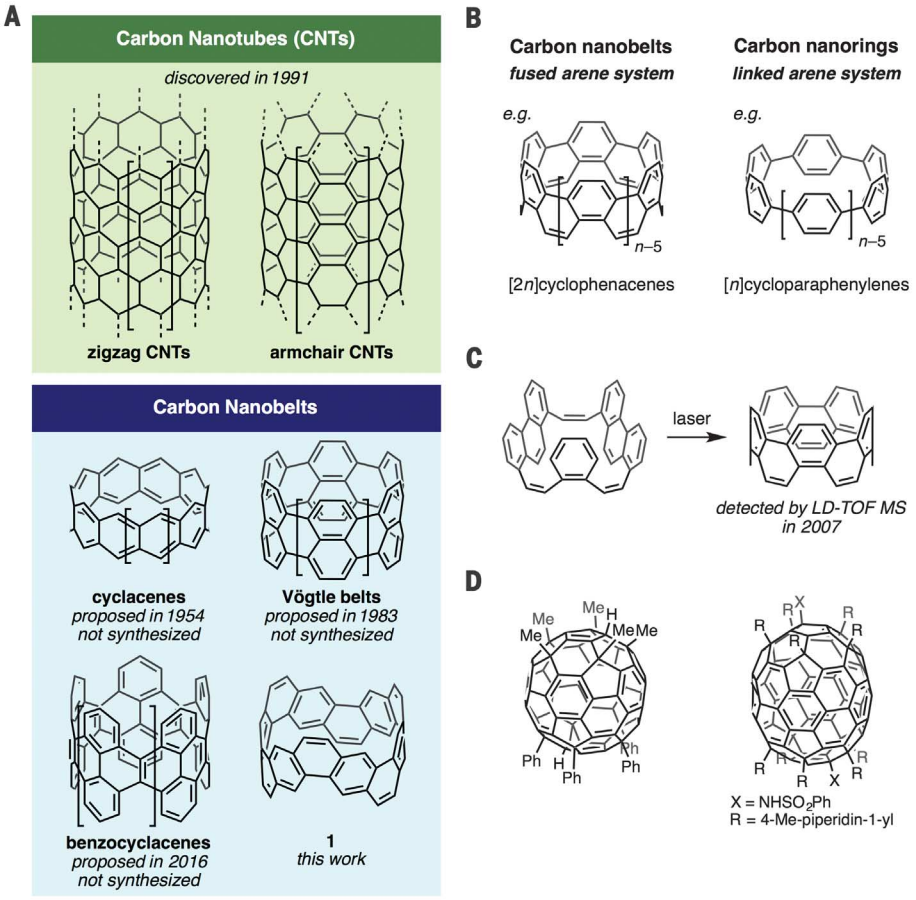

Fig. 1. Carbon nanotubes (CNTs) and carbon nanobelts. (**A**) Structures of CNTs and carbon nanobelts, where the square brackets show a repeating unit. (**B**) Difference between carbon nanobelts and carbon nanorings. (**C**) Mass detection of [12]cyclophenacene by Iyoda *et al.* (*11*). (**D**) Multiaddition to C_{60} and C_{70}, leading to the extraction of carbon nanobelt substructures. LD-TOF MS, laser desorption–time-of-flight mass spectrometry; Me, methyl; Ph, phenyl.

[1]JST-ERATO (Japan Science and Technology Agency, Exploratory Research for Advanced Technology) Itami Molecular Nanocarbon Project, Chikusa, Nagoya 464-8602, Japan. [2]Graduate School of Science, Nagoya University, Chikusa, Nagoya 464-8602, Japan. [3]Integrated Research Consortium on Chemical Sciences, Nagoya University, Chikusa, Nagoya 464-8602, Japan. [4]Institute of Advanced Energy, Kyoto University, Uji, Kyoto 611-0011, Japan. [5]Institute of Transformative Bio-Molecules (WPI-ITbM), Nagoya University, Chikusa, Nagoya 464-8602, Japan.
*Corresponding author. Email: ysegawa@nagoya-u.jp (Y.S.); itami@chem.nagoya-u.ac.jp (K.I.)

prepared in four steps from *p*-xylene (supplementary materials). A Wittig reaction then provided stilbene **5** with high *Z*-selectivity (*Z*:*E*, 20:1) owing to the *ortho*-bromo effect (*21*). Without isolation, **5** was subjected to a subsequent monodebromination (*22*) in the same pot to afford **6** in 80% yield from **3** after recrystallization. Repeating the same reaction sequence with **6** and **4** worked efficiently to furnish the trimer **7** with similar yields. Phosphonium formation followed by deprotection of dimethyl acetal with HCl produced the bifunctional unit **8**, which, after counterion exchange, could be recrystallized in excellent yields as a PF_6 salt. Treatment of a CH_2Cl_2 solution of **8** with *t*-BuOK (Bu, butyl) triggered a sequential cyclodimerization. The resulting macrocycle **2** could be isolated in multigram quantities after recrystallization from toluene, and the all-*Z* macrocyclic structure was unambiguously established by x-ray crystallography.

With precursor **2** in hand, we investigated the key aryl-aryl coupling reaction. Among the various conditions tested, the combination of $Ni(cod)_2$ (cod, 1,5-cyclooctadiene) and 2,2′-bipyridyl with a short reaction time furnished **1**. Under the optimal conditions—12 equivalents of $Ni(cod)_2$ and 2,2′-bipyridyl at 70°C for 15 min—pure **1** could be isolated as red crystals in 1% yield. Although this low yield leaves room for considerable improvement, the ability to prepare precursor **2** on a large scale permitted sufficient quantities of this long-sought carbon nanobelt **1** to be purified, isolated, and fully characterized. Nuclear magnetic resonance (NMR) analysis revealed two and four sets of nonequivalent protons and carbons, respectively, in accord with the D_{3d} symmetry of the molecule. The signals were attributed on the basis of two-dimensional NMR experiments and were in good agreement with calculated values (see the supplementary materials for details).

The structure of **1** was confirmed by x-ray crystallography (Fig. 3). Suitable crystals generated from a solution of *N*,*N*′-dimethylpropyleneurea, $CHCl_3$, and cyclohexane at room temperature gave a reliable x-ray crystal structure of **1** as **1**·3$CHCl_3$ [*R* factor = 0.0399; intensity $I > 2\sigma(I)$. As shown in Fig. 3, A and B, **1** has a belt-shaped structure (C_{2h} symmetry in crystal) with a diameter of 8.324 Å in which all benzene rings are fused. This is a distinct structural feature from previously reported carbon nanorings such as CPPs (*23*).

In the packing structure, individual molecules of **1** are separated from one another by chloroform molecules localized above, below, and outside them (Fig. 3, C and D). All crystallographically independent C–C bond lengths are shown in Fig. 3E. Judging from the short lengths of the C1–C1* and C5–C9 bonds, it appears that the resonance structure assigning them a double bond character (C=C is typically 1.337 Å) is the main contributor to the structure of **1** (Fig. 3F, upper structure). However, the C3–C3* and C7–C11 bonds are shorter than the bonds in [6]CPP linking the benzene rings [1.490(2) Å] (*23*), implying that ring **a** may also have a weak aromatic character (Fig. 3F, lower structure) as a minor resonance structure. Ring **b** appears to be more strongly aromatic, in accord with the small bond alternation around its circumference. These observations are in good agreement with the optimized structure of **1** predicted by DFT calculations. The nucleus-independent chemical shift (NICS) (*24*) values (ring **a**, –2.01; ring **b**, –7.45) also indicate substantial aromaticity of ring **b**.

For insight into the electronic structure of **1**, we investigated its photophysical properties (Fig. 4A). The optical absorption spectrum of **1** in CH_2Cl_2 solution presents two major bands at 284 and 313 nm. A smaller peak at 412 nm and a weakly absorbing region extending up to 500 nm are also observed. The absorption in the region between 450 and 500 nm could be attributed to a symmetry-forbidden HOMO (highest occupied molecular orbital) → LUMO (lowest unoccupied molecular orbital) transition (528 nm) with an oscillator strength (*f*) of 0.00 predicted by time-dependent DFT calculations at the B3LYP/6-31G(d) level of theory (Fig. 4D and supplementary materials). The weak absorption of the forbidden transition of **1** may be caused by structural rigidity, which prevents deformation away from high symmetry. The 412-nm absorption could be assigned to a combination of HOMO – 1 → LUMO and HOMO → LUMO + 1 transitions, which were calculated to absorb at 413 nm with weak oscillator strength (*f* = 0.08). Carbon nanobelt **1** exhibits a deep

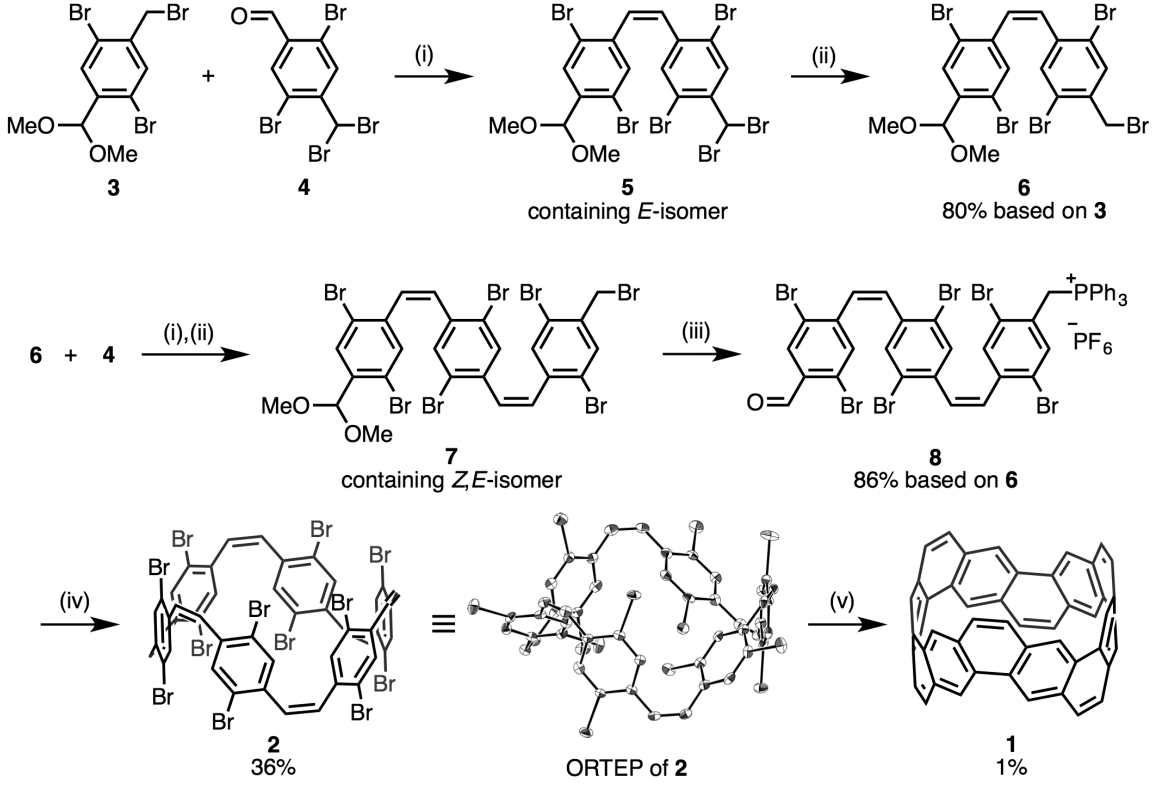

Fig. 2. Synthetic scheme to produce 1. Reaction conditions were as follows: (i) **3** or **6** (1.00 equiv), PPh_3 (1.04 equiv), THF/MeOH, reflux, 3 or 3.5 hours; **4** (1.02 equiv), *t*-BuOK (1 M in THF, 1.00 equiv), rt, 25 or 60 min. (ii) $(MeO)_2POH$ (1.30 equiv), *i*-Pr_2NEt (1.40 equiv), rt, 1 or 3 hours. (iii) PPh_3 (1.04 equiv), THF/MeOH, reflux, 5 hours; 4 M aqueous HCl, acetone, rt, 2 hours; KPF_6, CH_2Cl_2, rt, 3 min. (iv) *t*-BuOK (1 M in THF, 1.20 equiv), CH_2Cl_2, 0°C to rt, 80 min. (v) **2** (1.00 equiv), $Ni(cod)_2$ (12.0 equiv), 2,2′-bipyridyl (12.0 equiv), DMF, 70°C, 15 min. The Oak Ridge thermal-ellipsoid plot (ORTEP) of **2**·2toluene is shown at 50% probability, with hydrogen atoms and toluene molecules omitted for clarity. THF, tetrahydrofuran; cod, 1,5-cyclooctadiene; Pr, propyl; Et, ethyl; DMF, *N*,*N*-dimethylformamide; equiv, equivalent; rt, room temperature.

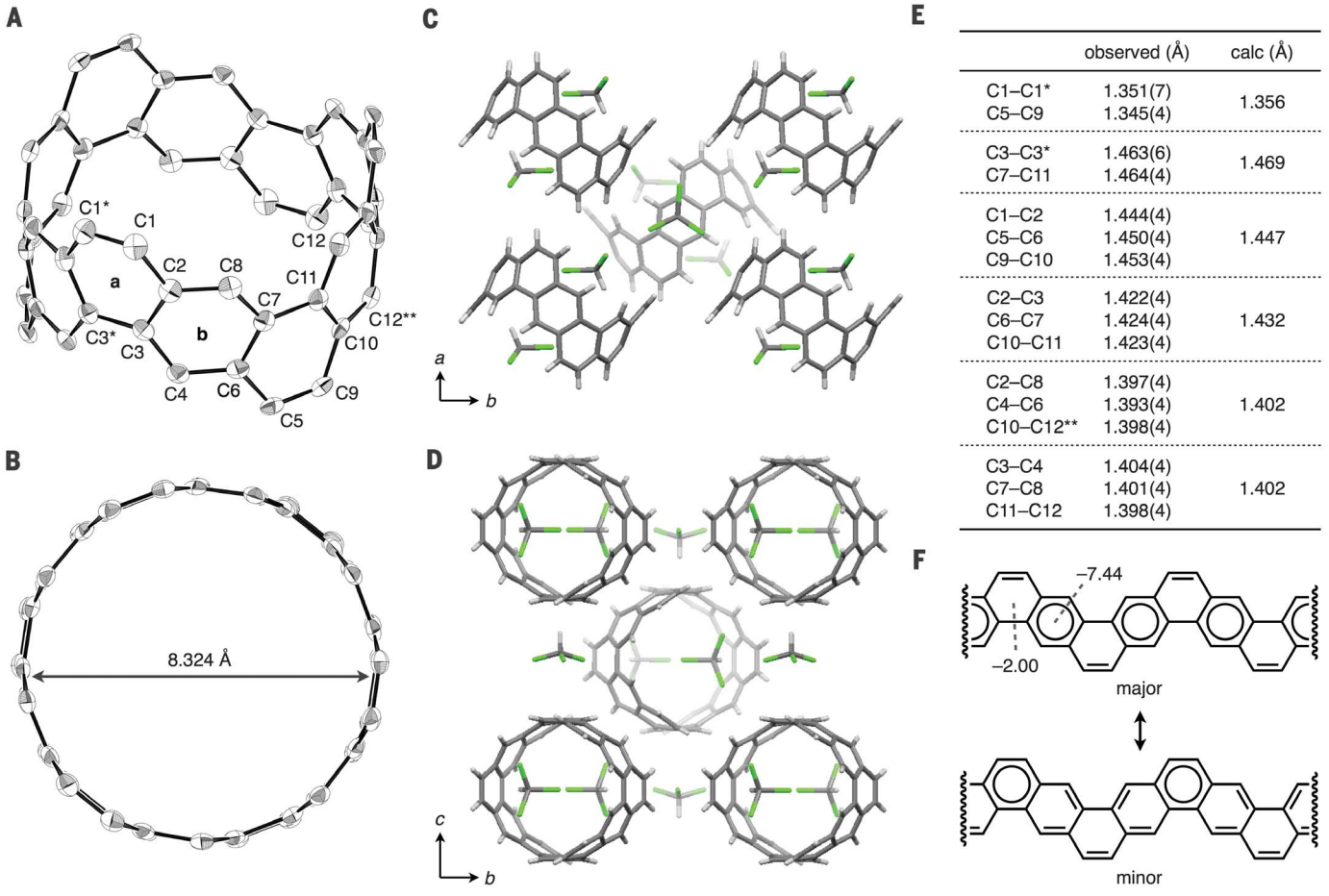

	observed (Å)	calc (Å)
C1–C1*	1.351(7)	1.356
C5–C9	1.345(4)	
C3–C3*	1.463(6)	1.469
C7–C11	1.464(4)	
C1–C2	1.444(4)	1.447
C5–C6	1.450(4)	
C9–C10	1.453(4)	
C2–C3	1.422(4)	1.432
C6–C7	1.424(4)	
C10–C11	1.423(4)	
C2–C8	1.397(4)	1.402
C4–C6	1.393(4)	
C10–C12**	1.398(4)	
C3–C4	1.404(4)	1.402
C7–C8	1.401(4)	
C11–C12	1.398(4)	

Fig. 3. Structural features of carbon nanobelt 1. (**A** and **B**) ORTEP diagram of **1**·3$CHCl_3$ at 50% probability with hydrogen atoms and solvent molecules omitted for clarity. A quarter of the entire structure constitutes an asymmetric unit; the carbons with one and two asterisks are in the second and the third asymmetric units, respectively. (**C** and **D**) Packing structures of **1** along the *c* and *a* axes (gray, carbon; white, hydrogen; green, chlorine). One of the disordered $CHCl_3$ molecules is shown for each position. (**E**) Bond lengths of **1**. Optimization for the calculated values was performed at the B3LYP/6-31G(d) level of theory. (**F**) Resonance structures of **1** with NICS(0) values calculated at the GIAO B3LYP/6-311+G(2d,p)//B3LYP/6-31G(d) level of theory. Clar aromatic sextets are shown with circles.

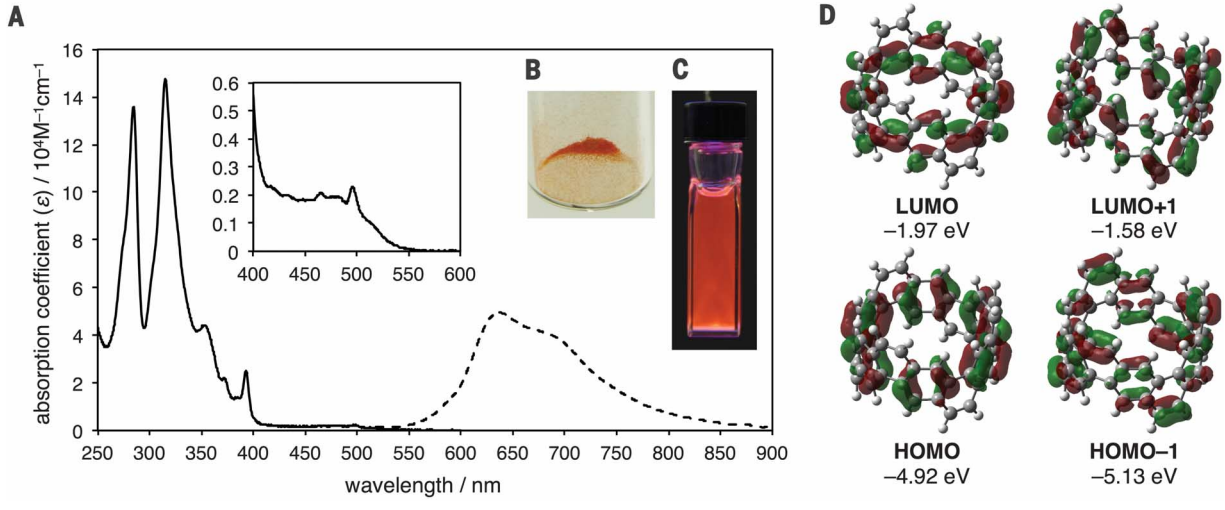

Fig. 4. Photophysical properties of carbon nanobelt 1. (**A**) Ultraviolet-visible absorption (solid line) and fluorescence (dashed line, normalized) spectra of the CH_2Cl_2 solution of **1**. Absorption coefficients were obtained at 5×10^{-6} M. A weakly absorbing region (inset) was measured at 7×10^{-5} M. The fluorescence spectrum was acquired after excitation at 500 nm. (**B**) Photograph of **1**·3$CHCl_3$ crystals. (**C**) Photograph of a CH_2Cl_2 solution of **1** irradiated at 365 nm. (**D**) Frontier molecular orbitals of **1** calculated at the B3LYP/6-31G(d) level of theory (isovalue, 0.003). Green and red, negative and positive wave functions, respectively; HOMO, highest occupied molecular orbital; LUMO, lowest unoccupied molecular orbital.

red fluorescence, easily visible in solution and in the solid state (Fig. 4, B and C, and supplementary materials). The fluorescence spectrum recorded upon excitation at 500 nm shows a broad emission band extending to the near infrared region with a maximum emission at 630 nm (Fig. 4A). Time-resolved measurements reveal a particularly long-lived excited state, both in CH_2Cl_2 solution (τ = 20.6 ns) and in the crystalline form (τ = 26.8 ns). The quantum yield (Φ = 3% in CH_2Cl_2 solution), with the classical relations $\Phi = k_r \times \tau$ and $\tau = 1/(k_r + k_{nr})$, gives the rates of nonradiative and radiative decay in solution ($k_{nr} = 4.8 \times 10^7\ s^{-1}$ and $k_r = 1.5 \times 10^6\ s^{-1}$, respectively), and the latter accords with a forbidden transition.

To compare **1** with extended CNTs, we measured the Raman spectrum of a single crystal of **1**·3$CHCl_3$ with laser excitation at 785 nm. The observed peaks were assigned to the corresponding vibration modes calculated at the B3LYP/6-31G(d) level of theory (see the supplementary materials for details). Among these peaks, the frequency corresponding to the radial breathing mode was 261 cm^{-1}, which is closer than that of [6]CPP (231 cm^{-1}) to the 287 cm^{-1} band (*25*) seen in (6,6)CNT (*26*). These observations support the structural rigidity of nanobelt **1** and its prospective interest as a model of (6,6)CNT.

The fully fused, fully conjugated, and rigid belt structure of **1** and its unusual optoelectronic properties bode well for a range of future applications in nanoelectronics and photonics. Just as the emergence of bowl-shaped corannulene (*27*) led to a rational, controlled synthesis of C_{60} (*28*) and opened the field of geodesic polyarenes (*29*), our synthesis of carbon nanobelt **1** could ultimately lead to the programmable synthesis of single-chirality, uniform-diameter CNTs (*30*–*32*) and open a field of nanobelt science and technology.

REFERENCES AND NOTES

1. D. Eisenberg, R. Shenhar, M. Rabinovitz, *Chem. Soc. Rev.* **39**, 2879–2890 (2010).
2. K. Tahara, Y. Tobe, *Chem. Rev.* **106**, 5274–5290 (2006).
3. S. Iijima, *Nature* **354**, 56–58 (1991).
4. E. Heilbronner, *Helv. Chim. Acta* **37**, 921–935 (1954).
5. F. H. Kohnke, A. M. Z. Slawin, J. F. Stoddart, D. J. Williams, *Angew. Chem. Int. Ed. Engl.* **26**, 892–894 (1987).
6. M. Standera, A. D. Schlüter, in *Fragments of Fullerenes and Carbon Nanotubes*, M. A. Petrukhina, L. T. Scott, Eds. (Wiley, 2012), pp. 343–366.
7. R. M. Cory, C. L. McPhail, A. J. Dikmans, J. J. Vittal, *Tetrahedron Lett.* **37**, 1983–1986 (1996).
8. K. Matsui, M. Fushimi, Y. Segawa, K. Itami, *Org. Lett.* **18**, 5352–5355 (2016).
9. F. Vögtle, A. Schroder, D. Karbach, *Angew. Chem. Int. Ed. Engl.* **30**, 575–577 (1991).
10. S. Kammermeier, P. G. Jones, R. Herges, *Angew. Chem. Int. Ed. Engl.* **35**, 2669–2671 (1996).
11. M. Iyoda, Y. Kuwatani, T. Nishinaga, M. Takase, T. Nishiuchi, in *Fragments of Fullerenes and Carbon Nanotubes*, M. A. Petrukhina, L. T. Scott, Eds. (Wiley, 2012), pp. 311–342.
12. B. L. Merner, L. N. Dawe, G. J. Bodwell, *Angew. Chem. Int. Ed.* **48**, 5487–5491 (2009).
13. L. T. Scott, *Angew. Chem. Int. Ed.* **42**, 4133–4135 (2003).
14. Y. Segawa, A. Yagi, K. Matsui, K. Itami, *Angew. Chem. Int. Ed,* **55**, 5136–5158 (2016).
15. F. E. Golling, M. Quernheim, M. Wagner, T. Nishiuchi, K. Müllen, *Angew. Chem. Int. Ed.* **53**, 1525–1528 (2014).
16. L. T. Scott *et al*., *J. Am. Chem. Soc.* **134**, 107–110 (2012).
17. E. Nakamura, K. Tahara, Y. Matsuo, M. Sawamura, *J. Am. Chem. Soc.* **125**, 2834–2835 (2003).
18. Y. Li, D. Xu, L. Gan, *Angew. Chem. Int. Ed.* **55**, 2483–2487 (2016).
19. Y. Segawa, A. Yagi, H. Ito, K. Itami, *Org. Lett.* **18**, 1430–1433 (2016).
20. D. Myśliwiec, M. Stępień, *Angew. Chem. Int. Ed.* **52**, 1713–1717 (2013).
21. E. C. Dunne, É. J. Coyne, P. B. Crowley, D. G. Gilheany, *Tetrahedron Lett.* **43**, 2449–2453 (2002).
22. P. Liu, Y. Chen, J. Deng, Y. Tu, *Synthesis* **2001**, 2078–2080 (2001).
23. J. Xia, R. Jasti, *Angew. Chem. Int. Ed.* **51**, 2474–2476 (2012).
24. P. R. Schleyer, C. Maerker, A. Dransfeld, H. Jiao, N. J. R. E. Hommes, *J. Am. Chem. Soc.* **118**, 6317–6318 (1996).
25. E. H. Hároz *et al*., *Phys. Rev. B* **91**, 205446 (2015).
26. M. Peña Alvarez *et al*., *Angew. Chem. Int. Ed.* **53**, 7033–7037 (2014).
27. W. E. Barth, R. G. Lawton, *J. Am. Chem. Soc.* **88**, 380–381 (1966).
28. L. T. Scott *et al*., *Science* **295**, 1500–1503 (2002).
29. Y.-T. Wu, J. S. Siegel, *Top. Curr. Chem.* **349**, 63–120 (2014).
30. M. F. L. De Volder, S. H. Tawfick, R. H. Baughman, A. J. Hart, *Science* **339**, 535–539 (2013).
31. J. R. Sanchez-Valencia *et al*., *Nature* **512**, 61–64 (2014).
32. Y. Segawa, H. Ito, K. Itami, *Nat. Rev. Mater.* **1**, 15002 (2016).

ACKNOWLEDGMENTS

This work was supported by the ERATO program of the JST (K.I.) and the Swiss National Science Foundation (Early Postdoc Mobility fellowship no. P2BEP2_158977 to G.P.). We thank T. Watanabe (Nagoya University) for the large-scale synthesis of **2**, N. Mitoma (Nagoya University) for measuring the Raman spectrum of **1**, H. Ito (Nagoya University) for assistance with quantum yield measurements and for taking photographs of **1**, and C. M. Crudden (Queen's University and Nagoya University) for fruitful discussion and critical comments. Computations were performed using the Research Center for Computational Science, Okazaki, Japan. ITbM is supported by the World Premier International Research Center Initiative (WPI), Japan. All the past and current members of the Itami group are greatly acknowledged for their support and encouragement during our decade-long campaign of ring, belt, and tube projects. We dedicate this paper to the memory of Fritz Vögtle, who pioneered the carbon nanobelt research. Crystallographic data for compounds **1** and **2** are available free of charge from the Cambridge Crystallographic Data Centre under CCDC identifiers 1524455 and 1524456, respectively (www.ccdc.cam.ac.uk/structures/). All authors are inventors on a patent application (JP2017-025127) submitted by Nagoya University that covers the synthesis of carbon nanobelts.

SUPPLEMENTARY MATERIALS

www.sciencemag.org/content/356/6334/172/suppl/DC1
Materials and Methods
Figs. S1 to S19
Tables S1 to S3
References (*33*–*46*)

20 January 2017; accepted 27 February 2017
10.1126/science.aam8158

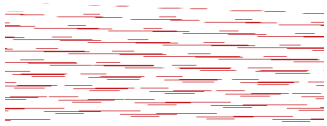

Synthesis of a carbon nanobelt
Guillaume Povie, Yasutomo Segawa, Taishi Nishihara, Yuhei Miyauchi and Kenichiro Itami (April 13, 2017)
Science **356** (6334), 172-175. [doi: 10.1126/science.aam8158]

Editor's Summary

Stitching a belt out of carbon rings

If you had a molecular scalpel, you could slice a carbon nanotube twice against the long axis to excise a loop of fused phenyl rings. Of course, knives don't come that small. Instead, Povie *et al.* succeeded in stitching together such a nanometer-scale belt in bottom-up fashion from molecular components, using consecutive Wittig reactions (see the Perspective by Siegel). The belt of 12 edge-sharing rings could ultimately be a first step toward more precisely controlled bottom-up syntheses of extended nanotubes.

Science, this issue p. 172; see also p. 135

Science (print ISSN 0036-8075; online ISSN 1095-9203) is published weekly, except the last week in December, by the American Association for the Advancement of Science, 1200 New York Avenue NW, Washington, DC 20005.